Formation of aligned nanosilicide structures in a MBE-grown Au/Si(110) system: a real-time temperature-dependent TEM study

2009 J. Phys.: Condens. Matter 21 205403

(http://iopscience.iop.org/0953-8984/21/20/205403)

J. Phys.: Condens. Matter **21** (2009) 205403 (7pp) doi:10.1088/0953-8984/21/20/205403

Formation of aligned nanosilicide structures in a MBE-grown Au/Si(110) system: a real-time temperature-dependent TEM study

Umananda M Bhatta[1], **J K Dash**[1], **Anupam Roy**[1,2], **A Rath**[1] and **P V Satyam**[1,3]

[1] Institute of Physics, Sachivalaya Marg, Bhubaneswar 751005, India
[2] Department of Materials Science, Indian Association for the Cultivation of Science, 2A&2B Raja S C Mullick Road, Kolkata 700032, Kolkata, India

E-mail: satyam@iopb.res.in and pvsatyam22@gmail.com

Received 1 February 2009, in final form 31 March 2009
Published 24 April 2009
Online at stacks.iop.org/JPhysCM/21/205403

Abstract

Thin Au films (∼2 nm) were deposited on an Si(110) substrate epitaxially under ultra-high vacuum (UHV) conditions in a molecular beam epitaxy (MBE) system. Real-time *in situ* transmission electron microscopy (TEM) measurements were carried out at various temperatures (from room temperature to 700 °C), which shows the formation and growth of aligned gold silicide nanorod-like structures. The real-time selected-area electron diffraction patterns show the presence of silicon and unreacted gold at lower temperatures (up to 363 °C), while at higher temperatures only the signature of silicon has been observed. The diffraction analysis from room temperature cooled systems show the presence of gold silicide structures. Around 700 °C, 97% of the nanostructures were found to be aligned nanosilicide-rod-like structures with a longer side of ≈37 nm and aspect ratio of 1.38. For a high temperature annealed system (at 600 °C), selected-area diffraction (SAD) and high resolution lattice (after cooling down to room temperature) confirmed the formation of nano-Au_5Si_2 structures. The alignment of gold silicide structures has been explained on the basis of lattice matching between the substrate silicon and silicide structures.

1. Introduction

The uppermost few atomic layers of a solid (known as the 'surface' of a solid) forms the interface of the solid with the surrounding environment. Not just being a static surface/interface, this is the home for a variety of ongoing atomic and molecular processes which are responsible for most of the important technologies on which our society depends today [1]. Gold is an interesting example of how surface effects throw up a lot of technological possibilities when one or more dimensions are reduced to below a critical length scale (for example, in gold nanomaterials). This noble metal has long been regarded as chemically inert in its bulk form. However, in the recent past it was found that Au in the 'nanocluster on metal oxide substrates' form exhibits very high catalytic activity for the partial oxidation of hydrocarbons, reduction of nitrogen oxides, etc [2–4]. Also, it has been observed that thiol-capped Au particles tend to show magnetism [5]. So, besides its importance in fundamental studies, study of such systems on oriented substrates are very relevant to many technological problems such as hetero-epitaxial growth of nanostructures, stability of catalysts, etc [6–8].

The interaction of metal films (including gold) with silicon has attracted considerable attention because of its importance in semiconductor technology. The formation of nanometal silicides, which are used as Schottky barriers and ohmic contacts in devices, are of particular interest in the emerging area of nanoscience and nanotechnology. The Au–Si binary phase diagram in the bulk system is well studied [9, 10] and

[3] Author to whom any correspondence should be addressed.

this system has a eutectic temperature around 363 °C with 81% gold and 19% Si composition. Formation of eutectic compounds has been explained by two basic mechanisms: (i) the formation of a supersaturated solid solution containing a large number of defects, giving rise to an increase of the free energy of the system, and hence the lower melting point and (ii) the formation of a transition epitaxial zone (without forming a solid solution), which leads to a decrease of lattice misfit. This in turn accounts for weakening of the bonds in the surface layers and the decrease in melting point [11]. Even though the structures of such eutectic alloys are well studied, the same thing cannot be said regarding the mechanism of eutectic alloy formation even in the bulk phase. The reason being the difficulty in obtaining experimental data on the structure of the interface during the formation of the eutectic alloy at the moment when the components pass from the solid to liquid state. With the increase in the interest in nanoscience, the alloy phase diagram for nanobinary systems such as nano-Au on Si poses new challenges and requires careful experimental and theoretical studies. There has been some amount of success in obtaining electron microscopic data due to the advent of heating-stage TEM holders. In this work, we present *in situ* high temperature TEM studies of the nano-Au–Si system.

The study of processes going on at the Si/metal interfaces at low temperatures have been well attempted by several groups [12–16]. It had been observed that the migration of Si atoms into Au and Pt took place at relatively lower temperatures (between 150 and 350 °C). Si–Pt, Si–Pd, Si–Ni and many other silicon–metal systems have been well studied by Mayer and Tu [17]. A detailed analysis by the authors indicated that the silicide formation in many such silicon–metal systems would end up in a silicon-rich phase. However, in some cases, they also found some intermediate phases which were metal-rich. Green and Bauer studied the formation of gold silicide phases for temperatures ranging from room temperature to 400 °C [18]. In their studies, about 10–100 nm gold films were evaporated onto an atomically cleaned Si(111) substrate under UHV conditions, showing the formation of three different gold silicide phases depending on film thickness, deposition temperature, annealing temperature and heating rate using the Auger electron spectroscopy (AES) and the low energy electron diffraction (LEED) methods. Le Lay reported the migration of Si to reduce the average gold concentration as the more probable process during low temperature thermal treatment ($\leqslant$400 °C) in Au–Si systems [19]. Baumann *et al* observed the precipitation of gold in silicon from a highly supersaturated solution and high temperature annealing studies based on high resolution TEM (HRTEM) showed the formation of small particles (10–20 nm diameter) consisting of metastable gold silicide [20].

Strained epitaxial layers are inherently unstable and such systems play an important role in semiconductor devices. Molecular beam epitaxy (MBE) is routinely used to grow such epitaxial layered systems in a controlled manner. The technique has advantages over the other deposition techniques from the fact that it has a precise control over beam fluxes and growth conditions. There have been a lot of interesting studies on the mechanism of relaxation of strain in such layers. Earlier, it was believed that the formation of dislocation was one of the means by which relaxation of strain occurs. However, in the past couple of decades the shape transition process has been shown to be the other alternative mechanism for strain relief. Tersoff and Tromp have given an analytical theory and shown that strained epitaxial islands, as they grow in size, may undergo a shape transition [21]. Experimental observations of shape transition during the growth of gold silicide islands on an Si(111) substrate were reported by Sekar *et al* [22]. In their studies, a 120 nm thick Au film was deposited under high vacuum conditions onto a bromine-passivated Si(111) substrate and annealed around the Au–Si eutectic temperature (363 °C). Below a critical size islands grew in the shape of equilateral triangles, following the symmetry of the Si(111) substrate [22]. However, at larger sizes, this symmetry ceases to exist and a shape transition takes place from triangle to trapezoid. Rout *et al* have reported the study of the growth of gold silicide microrods on an Si(110) substrate [23]. In these studies, a 45 nm thick Au film was deposited under high vacuum conditions on a bromine-passivated Si(110) substrate by thermal evaporation and annealed around the Au–Si eutectic temperature. Optical microscopy and scanning electron microscopy showed the growth of long wire-like gold silicide islands having facets. Preferential growth of these microrods along the [$\bar{1}$10] direction was attributed to lattice matching between gold silicide and silicon. These studies were carried out in a non-UHV environment and on uniform and thick gold layers deposited on passivated silicon substrates.

In this paper, we present the experimental observation of the growth of aligned gold silicide nanostructures during *in situ* thermal treatment in a TEM heating stage. About 2.0 nm thick gold was deposited on an atomically clean Si(110) substrate under UHV conditions. Morphological and structural changes were studied *in situ* at various temperatures in a transmission electron microscope (TEM). We will discuss the formation of gold silicide islands in the light of coincidence site lattice matching between substrate silicon and gold silicide. Detailed analysis has been carried out for size determination and shape variations at various temperatures.

2. Experimental details

For growing gold thin films on an atomically clean Si(110) surface a custom-made, compact MBE system has been used. More about the MBE system has been explained elsewhere [24]. N-type Si(110) substrates were loaded into the MBE chamber in which a base pressure $\approx 1.4 \times 10^{-10}$ mbar was achieved prior to deposition. Substrates were degassed at 600 °C for about 12 h inside the chamber and followed by flashing for about 3 min by direct heating at a temperature of $\approx$1200 °C. In this process, native oxide was removed and a clean Si(110) surface was obtained. On such ultra-clean surfaces, $\approx$2.0 nm thick gold was grown epitaxially by evaporating Au from a Knudsen cell, while keeping the substrates at room temperature (RT). Deposition rate was kept constant at 0.14 nm min^{-1}. During the growth, the chamber vacuum was $\approx 2.8 \times 10^{-10}$ mbar. The thickness monitor

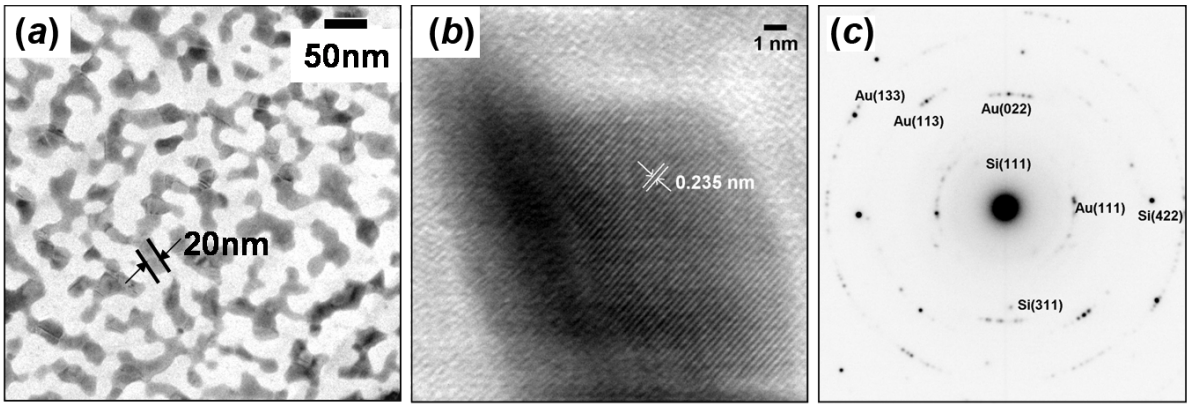

Figure 1. As-deposited MBE sample showing (a) gold nanostructures with typical size of about 20 nm, (b) corresponding high resolution image of one of the islands which is showing the d spacing of Au(111) and (c) SAD pattern showing reflections of both Si and Au.

was calibrated with Rutherford backscattering spectrometry (RBS) measurements. After the deposition, the sample was taken out of the MBE chamber and processed for planar TEM sample preparation. A disc of 3 mm diameter was cut using an ultrasonic disc cutter followed by lapping until it reached $\approx$100 μm thick. Using a dimple grinder, the sample was further thinned down to $\approx$25 μm thick at the centre of the sample. Finally, electron transparency was achieved through low energy Ar ion milling. TEM measurements were done with 200 keV electrons (2010, JEOL HRTEM). The sample was loaded in a (GATAN 628UHR) single-tilt heating holder. The heating stage has a tantalum furnace that can be used to heat the specimen up to 1000 °C. The temperature is measured by a Pt/Pt–Rh thermocouple and is accurate to within a couple of degrees. The holder has a water cooling system to avoid overheating of the sample surroundings and the specimen chamber, while keeping only the sample at a specified temperature. Real-time measurements were carried out using a CCD camera (GATAN 832) in which real-time movies can also be recorded at a grab rate of 25 frames s^{-1}.

3. Results and discussion

Figure 1(a) depicts bright-field (BF) TEM for a $\approx$2.0 nm thick Au film deposited on an Si(110) substrate. Connected gold structures were seen with 48% coverage of gold film. It is known that Au on Si growth was found to follow layer-by-island (Stranski–Krastanov, SK growth) growth. From the bright-field planar TEM, it is not possible to rule out the existence of a wetting layer. Figure 1(b) shows an HRTEM image from one of the gold nano-islands, which has a lattice spacing of (0.235 nm $\pm$ 0.005 nm) corresponding to Au(111) planar spacing. Figures 1 and 2 are the bright-field (BF) images and the contrast, i.e. black or white, in the bright-field image arises due to 'mass–thickness' contrast. Mass contrast arises from the incoherent elastic scattering (Rutherford) of electrons which strongly depends on Z, i.e. the mass or the density as well as the thickness of the specimen. As the mass and/or thickness of the specimen increases, there will be more elastic scattering because the mean free path remains fixed. So, in the case of a bright-field (BF) image, thicker and/or higher mass areas will appear darker than thinner and/or lower mass areas. The selected-area diffraction (SAD) from this system show the presence of the polycrystalline nature of un-reacted gold apart from a single-crystalline Si background (figure 1(c)). The individual island structure was found to be crystalline. But no aligned structures were observed in the as-deposited system. Typical size of the island structures was found to be $\approx$20 nm (figure 1(a)).

In situ heating temperatures were carried out with a ramp rate of 7 °C min^{-1}. At each set temperature, the specimen was kept for about 30 min after a stable temperature was achieved. No significant changes in morphology (through TEM imaging) or in crystallinity (through SAD) until 200 °C temperature were observed. As shown in figure 1(a), the gold islands have a connected network in the as-deposited system. Even at 200 °C, similar morphology was found. This shows the system was quite stable without any inter-diffusion among the gold nanostructures below 200 °C. Figure 2 depicts bright-field images at various temperatures (325, 350, 363, 400, 600 and 700 °C) and figure 3 shows SAD patterns taken at various temperatures (325, 363, 600 and 700 °C). Figure 2(a) depicts a BF image taken after the system was kept stable at 325 °C. Interestingly, the connected network starts breaking up and results in the in-plane diffusion of gold nanostructures. Isolated nanostructures of gold were formed at this temperature. The real-time SAD pattern at 325 °C (i.e. while the system was kept at this temperature) is shown in figure 3(a). The SAD pattern confirms the presence of silicon and unreacted gold in the system. It is well known that the Au–Si system has a eutectic phase at 363 °C. So the temperature was increased by smaller intervals (<25 °C) around the eutectic temperature. Figure 2(b) depicts the BF image taken at 350 °C. Interestingly, some rod-like structures started forming at quite a few places. As the temperature was increased to 350 and then to 363 °C (figure 2(c)), such places containing 'rod-like' nanostructures, started to grow in number. Furthermore, all these nanostructures appeared to get aligned along one particular direction. The SAD pattern taken at 363 °C (figure 3(b)) show the signature (compared to the case at 325 °C) of unreacted gold at this temperature. But the bright-field image (figure 2(c)) depicts many aligned nanostructures.

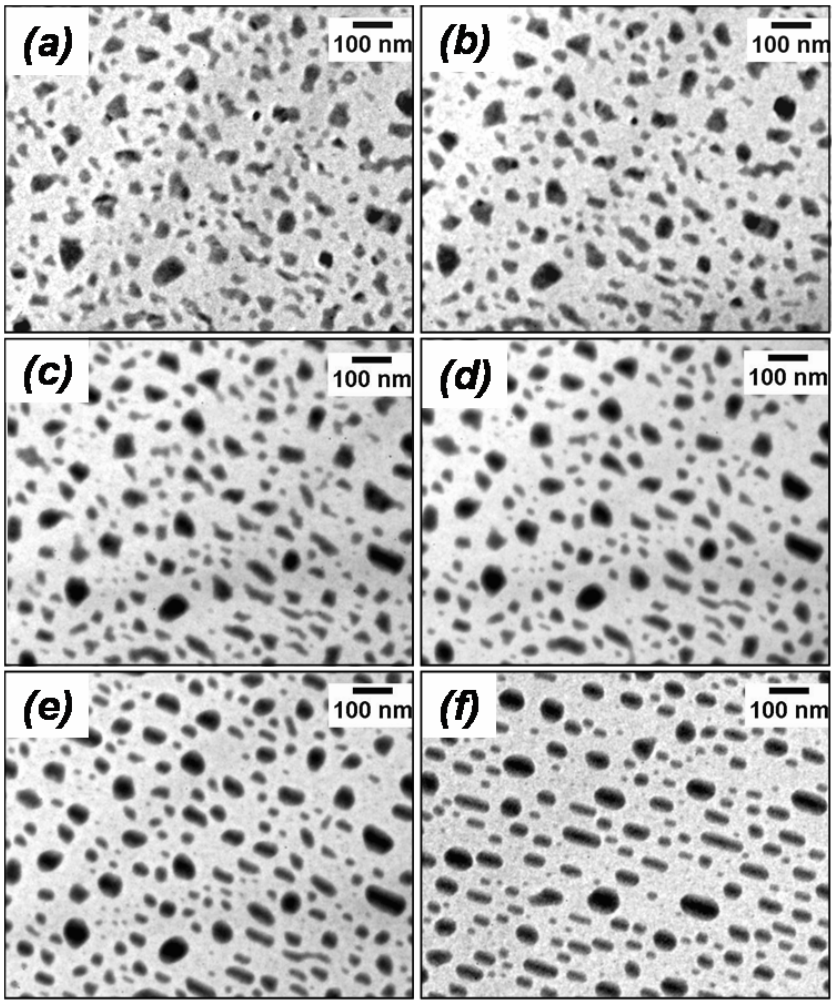

Figure 2. Bright-field transmission electron micrographs depicting real-time morphological changes during the *in situ* heating. (a), (b), (c), (d), (e) and (f) show the morphology at 325 °C, 350 °C, 363 °C, 400 °C, 600 °C and 700 °C, respectively. With increasing temperature growth of rod-like nanostructures can be seen aligned in one particular direction.

We have not taken an SAD pattern after cooling the specimen to room temperature at this stage and hence it is not possible to comment on eutectic phase formation. But from the shapes, there appears to be a high probability of forming eutectic nanosilicides at this temperature. More detailed studies at these low temperatures are in progress and will be discussed at a later stage elsewhere. It is important to note the studies by Ijima *et al*, on the dynamic behaviour of ultra-fine gold particles (∼2 nm) at atomic resolution using an HRTEM equipped with a real-time video facility [25]. They observed that particles continually change their shapes, orientations and internal atomic arrangements within a time interval of one-tenth of a second. The *in situ* diffraction pattern was found to be diffused, giving an impression that the particles are in a liquid phase. But, after cooling down to room temperatures, high resolution TEM showed a regular arrangement of atoms in individual particles [25]. In our studies, at lower temperatures (<363 °C), gold nanostructures were relatively stable at these temperatures.

Real-time *in situ* heating measurements were carried out at 400 °C (BF image at figure 2(d)), 600 °C (figure 2(e)) and 700 °C (figure 2(f)). More and more aligned nanostructures were formed at these higher temperatures. The average ratio of length to breadth, known as the 'aspect ratio', has been determined by using many bright-field images taken at each temperature: 325, 350, 363, 400, 600 and 700 °C. In determining the aspect ratios, the length was taken along the direction along which all the nanostructures were found to align at 700 °C. The average length, average aspect ratio and number of elongated nanostructures aligned along the particular direction (with reference to 700 °C) at various temperatures are tabulated in table 1. At 325 °C, the aspect ratio was found to be 1.04 and the average size along the length of these nanostructures was about 30.4 nm ± 1.4 nm. Interestingly, even at this stage some kind of alignment is seen (about 59% of the nanostructures having an aspect ratio of more than 1.0 along the aligned direction). As the temperature was increased, average aspect ratio increased and so was the number of aligned nanostructures per unit area. At 400 °C this ratio was found to be 1.16, with an average length about 32.3 ± 1.3 nm. The number of nanostructures with aspect ratio > 1 along the preferred direction had gone up to 80%. At 400

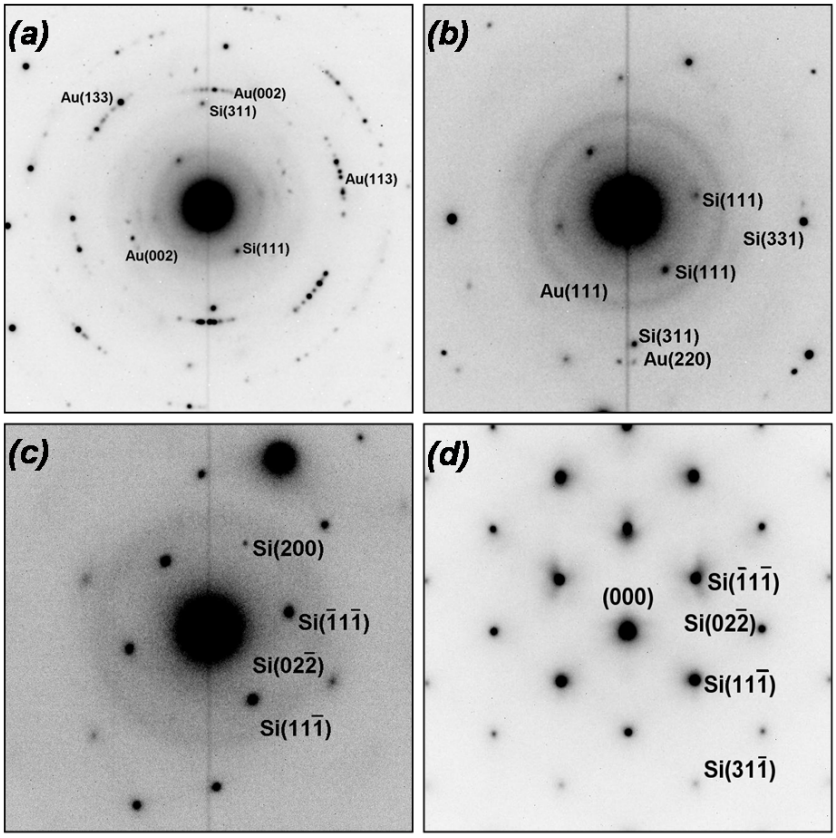

Figure 3. Real-time SAD patterns taken at various temperatures during heating, showing the presence of silicon reflections alone at higher temperatures. (a), (b), (c) and (d) show the real-time diffraction pattern at 325 °C, 363 °C, 600 °C and 700 °C, respectively.

and 600 °C, we did not observe any significant changes in the aspect ratio. But, at 700 °C, the aspect ratio increased to 1.38, with the coverage area increasing to 97.5%. The average length along the longer side was found to be 37.4±2.0 nm. We believe that this could be due to a possible structural phase transition from the eutectic phase (i.e. Au_4Si) at lower temperatures to Au_5Si_2 at higher temperatures. This appears to be the case as the *bulk* Au–Si phase diagram shows the requirement of ≈600 °C for Au_5Si_2 phase formation. Even as a monotonic increase in the average length and the defined aspect ratio was observed, careful observation through all the figures of figure 1 reveals that there is no large scale coalescence of these nanostructures while forming these aligned patterns. Most of the irregular structures found at lower temperatures (∼325 °C) undergo a structural transformation towards a regular shaped (rod-like) aligned nanostructure. We feel that there is a need to focus on an understanding of the phase diagram for nano-gold systems. We propose to do further studies to work on phase diagram for the nano-gold on silicon systems.

Careful observation reveals that initially, in spite of nanostructures having a rod-like shape and alignment in one direction, these structures have very rough edges and corners. With increasing temperatures smoothening of these edges and corners was observed. Ressel *et al* have reported about the behaviour of liquid Au–Si alloys on Si surfaces. ≈2.0 nm of gold was deposited on Si(111) and Si(100) substrates at 400 °C under UHV conditions to form the droplets [26]. The shape of the droplets changed from circular to hexagonal above 750 °C for the Au/Si(111). But, in the case of Au/Si(100), droplets were octagonal when solid and on melting became rounded at higher temperatures. The authors attributed this to the anisotropy in the line tension between the solid/liquid/gas line. With increasing temperature the entropic effects reduce the free energy difference between straight and curved steps, leading to a rounding of the shape.

Table 1. Average length of the nanostructures along the aligned direction, the aspect ratio and the percentage of ordering with given aspect ratio at various temperatures is mentioned in the table. With increasing temperature the ratio as well as mean size increases.

Temperature (°C)	Average length (in nm)	Average ratio	Percentage of elongated structures (%)
325	30.4 ± 1.4	1.04 ± 0.01	59
350	31.1 ± 1.4	1.08 ± 0.02	70
363	34.2 ± 1.0	1.11 ± 0.01	79
400	32.2 ± 1.4	1.18 ± 0.02	80
600	34.0 ± 1.2	1.23 ± 0.02	82
700	37.4 ± 2.0	1.37 ± 0.02	97

We discuss the alignment of structure in the nano-gold silicide in the following. The growth along the [110] direction could be related to directional anisotropy nucleation and growth. Roeder *et al* observed the formation of one-dimensional Cu chains on a Pd(110) surface [27]. In the case of Cu/Pd(110) migration barriers are 0.76 eV and 0.51 eV for the two orthogonal directions [001] and [1$\bar{1}$0],

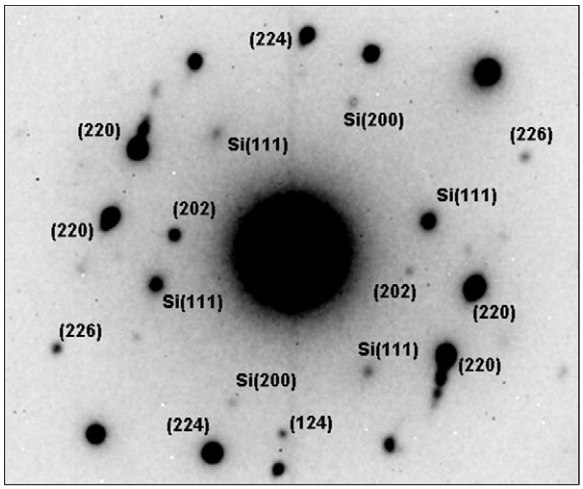

Figure 4. Selected-area diffraction taken at room temperature after the sample was heated up to 600 °C, showing presence of Au_5Si_2.

Table 2. Comparison of Au_5Si_2 *d* spacing as obtained by our group to that of Tsaur *et al* [30].

$Au_5Si_2(hkl)$	*d* (our observation) (nm)	*d* (Tsaur *et al*) (nm)
202	0.364 ± 0.005	0.362
302	0.252 ± 0.005	0.255
220	0.235 ± 0.005	0.234
130	0.223 ± 0.005	0.226
224	0.203 ± 0.005	0.2006
403	0.191 ± 0.005	0.1903
226	0.173 ± 0.005	0.1725

respectively. This difference gives rise to faster growth along the $[1\bar{1}0]$ direction. Yinggang Li *et al* proposed a model to provide an explanation for this result [28]. The model predicts a transition from roughly isotropic islands at very low temperature to one-dimensional linear island structures at moderate temperature, which corresponds to the onset of 'anisotropic corner rounding'. The migration barrier experienced by the gold atoms along the length of a needle and around the corners along (two orthogonal directions) differ. This has been explained as due to the different bonding strengths along two facets [29]. Our results are also in line with the results of Roeder *et al* [27] and the model proposed by Yinggang Li *et al* [28].

In the following, we discuss the SAD and HRTEM results that are obtained for a system cooled to room temperature from 600 °C. As mentioned previously, though the aligned nanostructures formed at high temperatures, real-time SAD patterns showed the presence of single-crystalline silicon only. The sample was cooled down to room temperature from 600 °C and selected-area diffractions were taken to look for the crystalline nature of these well-aligned nanostructures. Apart from single-crystalline silicon reflections, a few extra spots were also found which did not match with silicon (figure 4). Interestingly, as mentioned earlier, no spots other than that of pure silicon were seen for real-time SAD at 600 °C (figure 3(c)). As discussed earlier by Ijima *et al* continuous changes in the internal atomic arrangements of ultra-fine gold

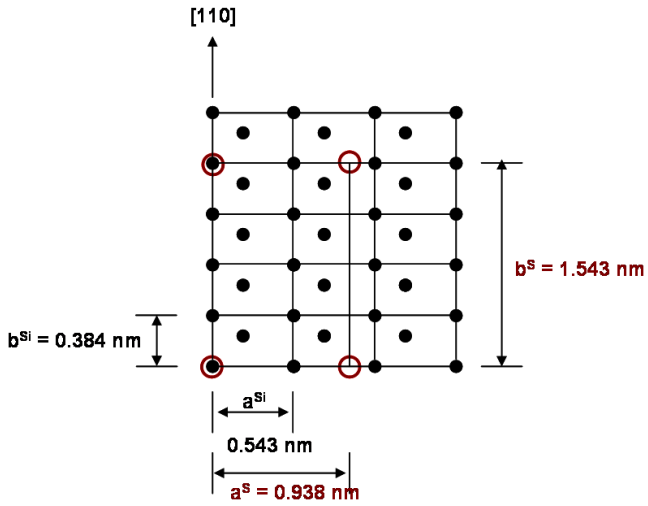

Figure 5. Possible structural relationship between Si (●) and gold silicide (○) for Au_5Si_2 phase. Here, a^{Si} and b^{Si} are the lattice vectors corresponding to the Si lattice (●). a^S and b^S are the lattice vectors corresponding to the Au_5Si_2 lattice (○). Approximate lattice matching along [110] would produce smaller strain influencing the elongated island growth along this easy axis.

(This figure is in colour only in the electronic version)

nanoparticles contribute to the diffused SAD pattern. But here, the size of the gold particles was much more than what has been described by the above authors and the melting point of particles of such a size is also close to the bulk value (≈1000 °C). So, figure 3(c) should have shown reflections due to gold as well. Absence of any such reflections again strongly suggests that there has already been a phase transformation to Au–Si nanosilicide at much lower temperatures (around 363 °C). After cooling to room temperature, one of the reflections showed a *d* spacing of 0.364 nm ± 0.005 nm, which is much higher than the Si(111) reflection (≈0.313 nm). Several other reflections were also found which were different from that of pure single-crystalline silicon or from pure gold. Detailed analysis showed that all these extra reflections would match quite well with the non-eutectic (forms at ≈635 °C) hexagonal phase of Au_5Si_2 [30]. Measured inter-planar-spacing (*d*) values and comparative values obtained by Tsaur *et al* [30] are shown in table 2. We confirm the formation of nano-gold-silicide structures using the SAD results. The lattice matching between the substrate silicon and silicide structures can also be used to explain the aligned structures. In thicker non-UHV-grown gold films on bromine-passivated Si(110) substrates, Rout *et al* observed the formation of well-aligned microrods on similar systems. The major cause of such elongated islands was attributed to the relaxation of strain that is associated with hetero-epitaxial growth. They obtained a silicide composition (17% Si, 83% Au) which is close to the eutectic composition. In our case, we see the formation of Au_5Si_2 that can also be understood using similar arguments. Hexagonal Au_5Si_2 (gold silicide) structure has a unit cell with $a^S = 0.938$ nm and $c^S = 1.545$ nm. On an Si(110) surface, a rectangular unit cell is defined as $a^{Si} = 0.543$ nm (||[001]) and $b^{Si} = 0.384$ nm (||[110]) (figure 5). For the epitaxial growth on an Si(110) surface, the fact that $4b^{Si} \approx c^S$ (0.5% difference)

and the lattice matching is worse (a^{S} is 14% smaller than $2a^{Si}$ and c^{S} is 5% smaller than $3a^{Si}$) in the other directions [001] would cause growth in one direction (along b^{Si}), and the strain relief would favour the growth of elongated islands along the [110] direction and this is evident here in our results.

4. Summary

We have investigated the real-time temperature-dependent *in situ* TEM studies of nano-gold structures grown on clean Si(110) substrates. As-deposited gold films show well-connected nanostructures and at higher temperatures the gold nanostructures get isolated (around 300 °C). At 700 °C, aligned nanostructures were observed. SAD patterns and HRTEM imaging confirm the formation of gold silicide structures.

References

[1] Rosei F 2004 *J. Phys.: Condens. Matter* **16** S1373–436
[2] Valden M, Lai X and Goodman D W 1998 *Science* **281** 1647
[3] Haruta M 1997 *Catal. Today* **36** 153
[4] Wahlström E, Lopez N, Schaub R, Thostrup P, Rønnau A, Africh C, Lægsgaard E, Nørskov J K and Besenbacher F 2003 *Phys. Rev. Lett.* **90** 026101
[5] Crespo1 P, Litrán R, Rojas T C, Multigner M, de la Fuente J M, Sánchez-López J C, García M A, Hernando A, Penadés S and Fernández A 2004 *Phys. Rev. Lett.* **93** 087204
[6] Besenbacher F 1996 *Rep. Prog. Phys.* **59** 1737
[7] Rosei F and Rosei R 2002 *Surf. Sci.* **500** 395
[8] Rosei F and Rosei R 2003 *Science Technology and Education of Microscopy: an Overview* vol 1, ed A Méndez-Vilas (Badajoz: Formatex Center) p 24
[9] Hansen M, Anderko K and Salzberg H W 1958 *J. Electrochem. Soc.* **105** 260C
[10] Chen H S and Turnbull D 1967 *J. Appl. Phys.* **38** 3646
[11] Zalkin V M 1987 *The Nature of Eutectic Alloys and Contact Melting Effect* (Moscow: Metallurgy)
[12] Hiraki A, Nicolet M A and Mayer J W 1971 *Appl. Phys. Lett.* **18** 178
[13] Narusawa T, Komiya S and Hiraki A 1973 *Appl. Phys. Lett.* **22** 389
[14] Hiraki A, Lugujjo E and Mayer J W 1972 *J. Appl. Phys.* **43** 3643
[15] Hiraki A, Shuto K, Kim S, Kammura W and Iwami M 1977 *Appl. Phys. Lett.* **31** 611
[16] Iwami M, Kim S, Kammura W and Hiraki A 1980 *Japan. J. Appl. Phys.* **1** 489
[17] Mayer J W and Tu K N 1974 *J. Vac. Sci. Technol.* **11** 86
[18] Green A K and Bauer E 1974 *J. Appl. Phys.* **47** 1286
[19] Le Lay G 1983 *Surf. Sci.* **132** 169
[20] Baumann F H and Schroeter W 1988 *Phil. Mag. Lett.* **57** 75
[21] Tersoff J and Tromp R M 1993 *Phys. Rev. Lett.* **70** 2782
[22] Sekar K, Kuiri G, Satyam P V, Sundaravel B, Mohapatra D P and Dev B N 1995 *Phys. Rev.* B **51** 14330
[23] Rout B, Sundaravel B, Das A K, Ghose S K, Sekar K and Mahapatra D P 2000 *J. Vac. Sci. Technol.* B **18** 1847
[24] Goswami D K, Satpati B, Satyam P V and Dev B N 2003 *Curr. Sci.* **84** 903
[25] Ijima S and Ichihashi T 1986 *Phys. Rev. Lett.* **56** 616
[26] Ressel B, Prince K C, Homma Y and Heun S 2003 *J. Appl. Phys.* **93** 3886
[27] Roeder H, Hahn E, Brune H, Bucher J and Kern K 1993 *Nature* **366** 141
[28] Li Y, Bartelt M C, Evans J W, Waelchli N, Kampshoff E and Kern K 1993 *Phys. Rev.* B **56** 12539
[29] McCarthy D N and Brown S A 2008 *J. Phys.: Conf. Ser.* **100** 072007
[30] Tsaur B Y and Mayer J W 1981 *Phil. Mag.* A **43** 345